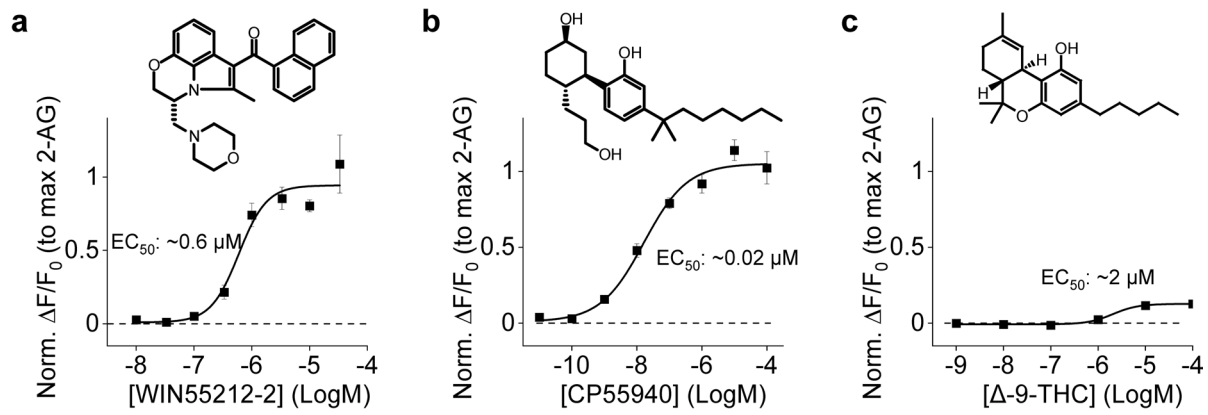
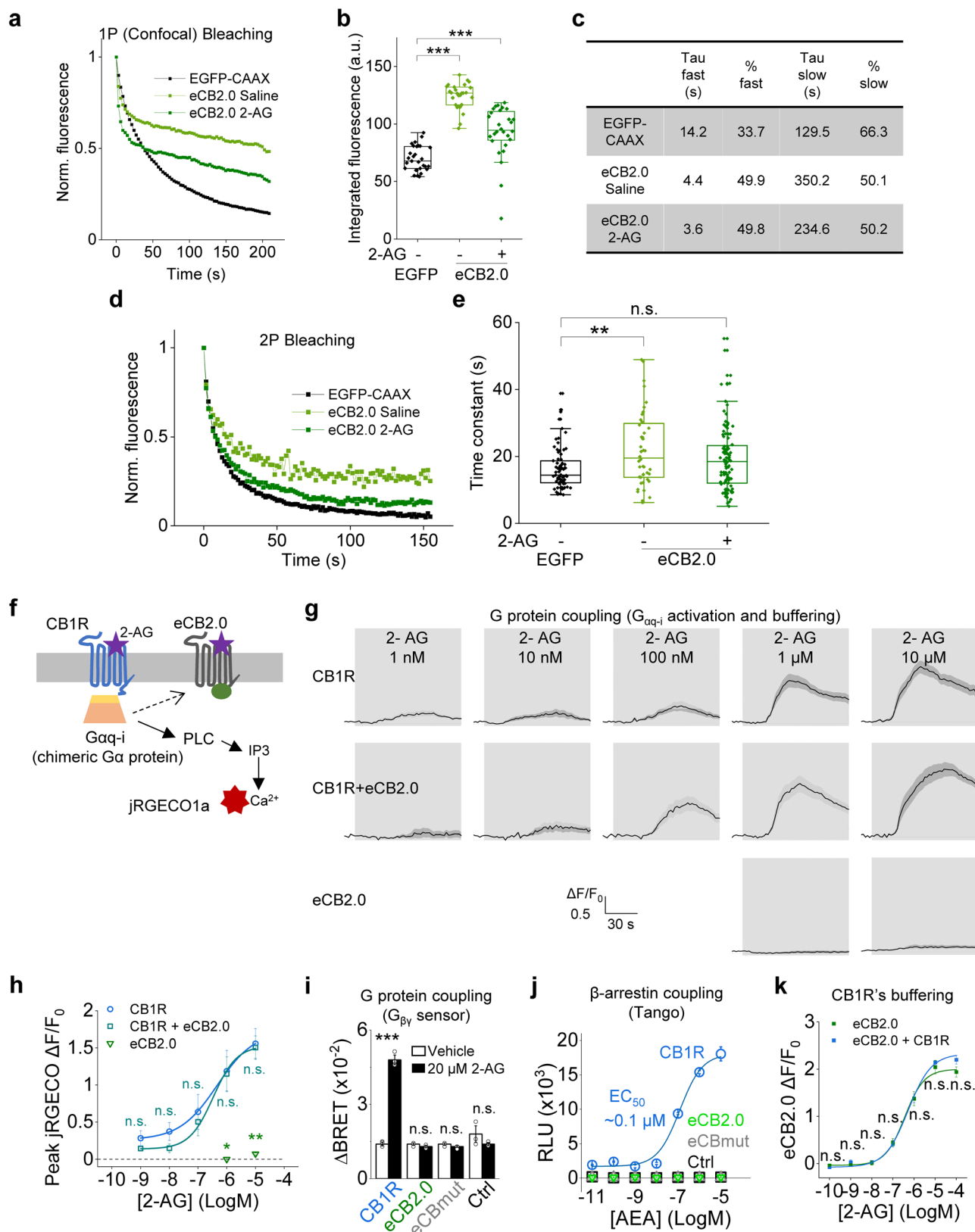


Extended Data Fig. 1 | Strategy for optimizing and screening the GRAB_{eCB} sensors. a, A flowchart showing the development process of the eCB2.0 sensor. Responses to 10 μM 2-AG of candidate sensors were shown alongside each step. **b**, Schematic diagram depicting the structure of the GRAB_{eCB2.0} sensor. The IgK leader sequence and the sequence derived from GRAB_{NE} are shown. **c**, Amino acids sequence of the eCB2.0 sensor. The phenylalanine residue at position 177^{2.64} in the CB1R was mutated to an alanine to generate the eCBmut sensor (indicated by the gray box). Note that the numbering used in the figure corresponds to the start of the IgK leader sequence.

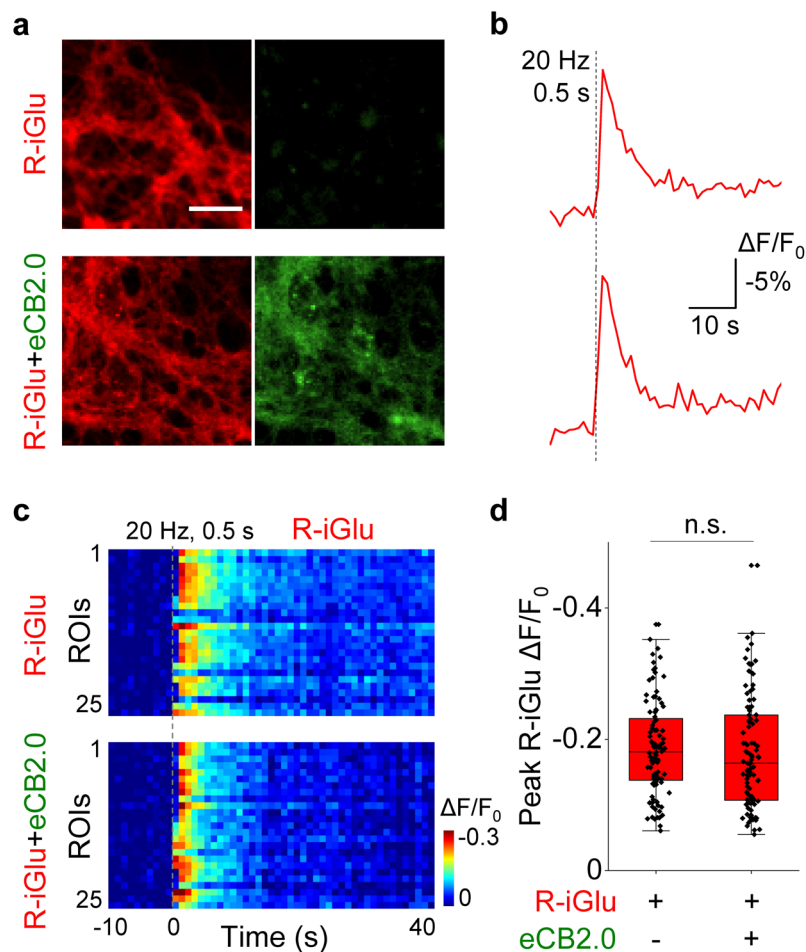


Extended Data Fig. 2 | Dose-response curves of GRAB_{eCB2.0} to synthetic CB1R agonists and the phytocannabinoid Δ -9-THC. **a, Dose-response curve of eCB2.0 to WIN55212-2; n = 3 wells each, mean \pm s.e.m. **b**, Dose-response curve of eCB2.0 to CP55940; n = 3 wells each, mean \pm s.e.m. **c**, Dose-response curve of eCB2.0 to Δ -9-THC; n = 3 wells each, mean \pm s.e.m.**

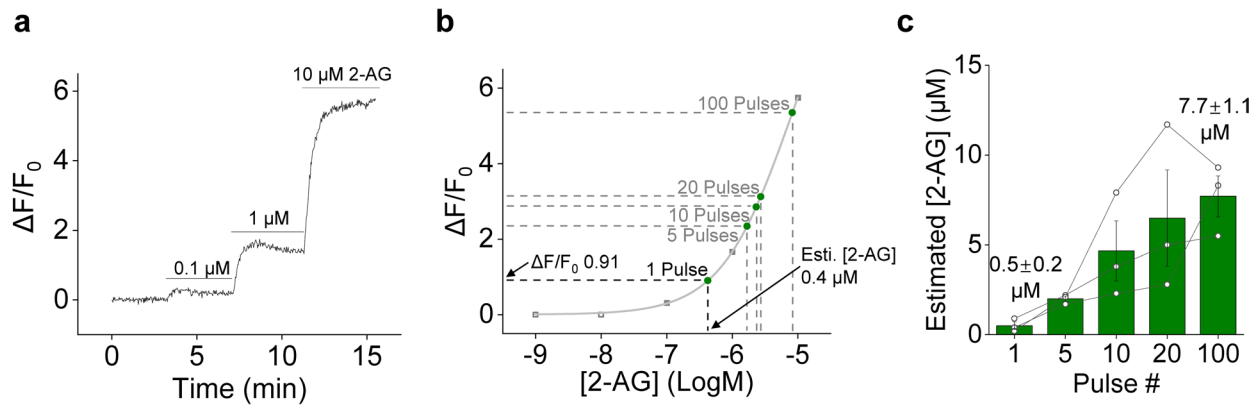


Extended Data Fig. 3 | See next page for caption.

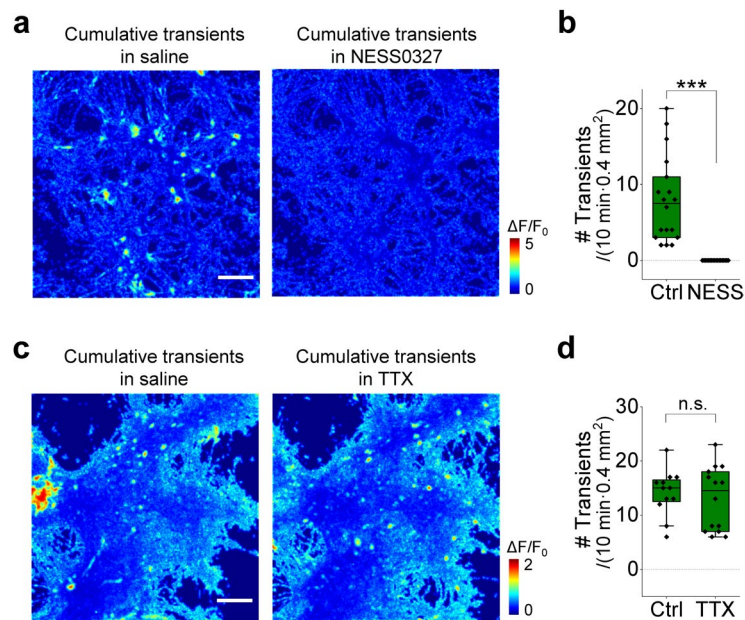
Extended Data Fig. 3 | Photostability and intracellular signaling couplings of GRAB_{eCB2.0} sensor. **a**, Normalized fluorescence of EGFP-CAAX and eCB2.0 (in the absence and presence of 2-AG) in HEK293T cells during 1P (confocal) bleaching. **b**, Integrated fluorescence of EGFP-CAAX and eCB2.0 (in the absence and presence of 2-AG) shown in **a**; $n = 29, 27, 28$ cells from 3 cultures. Boxes show the first and third quartiles as well as the median (line), and the whiskers extend to the most extreme data point that is no more than 1.5 \times the interquartile range from the box. Two-tailed Mann-Whitney tests were performed: $P = 1.44E-10$ (between EGFP and eCB2.0 in saline) and $1.37E-6$ (between EGFP and eCB2.0 with 2-AG). **c**, Fast and slow time constants and slow component amplitudes of EGFP-CAAX and eCB2.0 (in the absence and presence of 2-AG) traces fit by double exponentials. **d**, Normalized fluorescence of EGFP-CAAX and eCB2.0 (in the absence and presence of 2-AG) in HEK293T cells during 2P bleaching. **e**, Time constants of EGFP-CAAX and eCB2.0 (in the absence and presence of 2-AG) traces fit by single exponentials; $n = 79, 48, 104$ cells from 3 cultures. Boxes show the first and third quartiles as well as the median (line), and the whiskers extend to the most extreme data point that is no more than 1.5 \times the interquartile range from the box. Two-tailed Mann-Whitney tests were performed: $P = 0.0049$ (between EGFP and eCB2.0 in saline) and 0.0581 (between EGFP and eCB2.0 with 2-AG). **f**, Schematic diagram depicting the strategy for measuring G protein activation using the chimeric $G\alpha_{q-i}$ protein. **g**, Representative traces showing the jRGECO1a responses to 2-AG perfusion in cells expressing CB1R, CB1R + eCB2.0 or eCB2.0. **h**, Dose-response curves of peak jRGECO1a $\Delta F/F_0$ measured in cells expressing CB1R, CB1R + eCB2.0, or eCB2.0; $n = 4, 4$ and 3 cultures, mean \pm s.e.m. Two concentrations of 2-AG were used for eCB2.0 expressed cells. Two-tailed Student's *t* tests were performed: $P = 0.2392, 0.1455, 0.6711, 0.9191$ and 0.8371 (between CB1R and CB1R + eCB2.0); $P = 0.0156$ and 0.0015 (between CB1R and eCB2.0). **i**, G protein coupling was measured using a BRET $G_{\beta\gamma}$ sensor in cells expressing CB1R, eCB2.0, or eCBmut; $n = 3$ experiments, mean \pm s.e.m. Two-tailed Student's *t* tests were performed: $P = 3.84E-05, 0.4082, 0.0699$ and 0.2961 . **j**, β -arrestin coupling was measured using the Tango assay in cells expressing CB1R, eCB2.0, or eCBmut; $n = 3$ wells each, mean \pm s.e.m. **k**, Dose-response curves of eCB2.0 to 2-AG measured in cells expressing eCB2.0 or eCB2.0 + CB1R; $n = 3$ wells each, mean \pm s.e.m. Two-tailed Student's *t* tests were performed: $P = 0.3036, 0.3231, 0.7697, 0.7900, 0.9723, 0.5482$ and 0.1383 . ***, $p < 0.001$; **, $p < 0.01$; *, $p < 0.05$; n.s., not significant.



Extended Data Fig. 4 | Expression of GRAB_{eCB2.0} has no significant effect on electrically evoked glutamate release in cultured neurons. **a**, Fluorescence microscopy images of neurons expressing R^{nCP}-iGluSnFR (upper) and neurons co-expressing R^{nCP}-iGluSnFR and eCB2.0 (bottom). Similar results were observed for more than 20 neurons. Scale bar, 30 μ m. **b**, Example traces showing the electrical stimulation evoked glutamate signals. **c**, Pseudocolor change in R^{nCP}-iGluSnFR fluorescence in neurons expressing R^{nCP}-iGluSnFR (upper) and co-expressing R^{nCP}-iGluSnFR and eCB2.0 (bottom) before and after the electrical stimulation. Shown are 25 regions of interest (ROIs) in one culture each. **d**, Summary of peak R^{nCP}-iGluSnFR $\Delta F/F_0$ measured in neurons expressing R^{nCP}-iGluSnFR (upper) or co-expressing R^{nCP}-iGluSnFR and eCB2.0 (bottom); $n = 100$ ROIs from 4 cultures each. Boxes show the first and third quartiles as well as the median (line), and the whiskers extend to the most extreme data point that is no more than 1.5 \times the interquartile range from the box. Two-tailed Mann-Whitney test was performed: $P = 0.2564$. n.s., not significant.

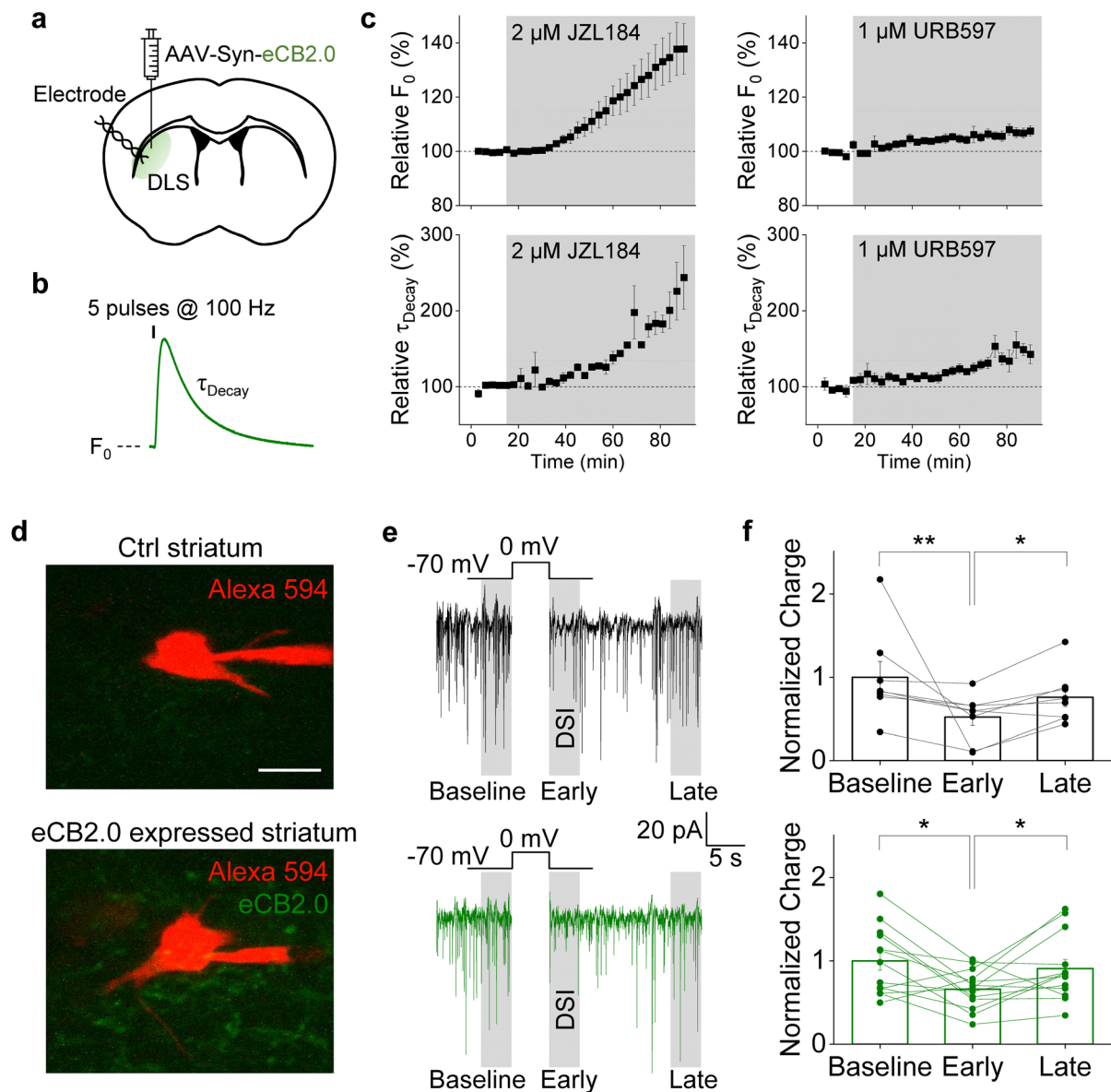


Extended Data Fig. 5 | Estimated concentrations of electrically evoked 2-AG release in cultured neurons. **a**, An example trace of $\Delta F/F_0$ measured in eCB2.0 expressed neurons; the indicated concentrations of 2-AG were applied. **b**, An example dose-response curve measured in neurons expressing eCB2.0. eCB2.0 signals evoked by 1–100 electrical pulses at 20 Hz and corresponding estimated 2-AG concentrations were indicated (green dots). **c**, Summary of estimated 2-AG release concentrations evoked by 1–100 electrical pulses at 20 Hz; $n=3$ cultures, mean \pm s.e.m.

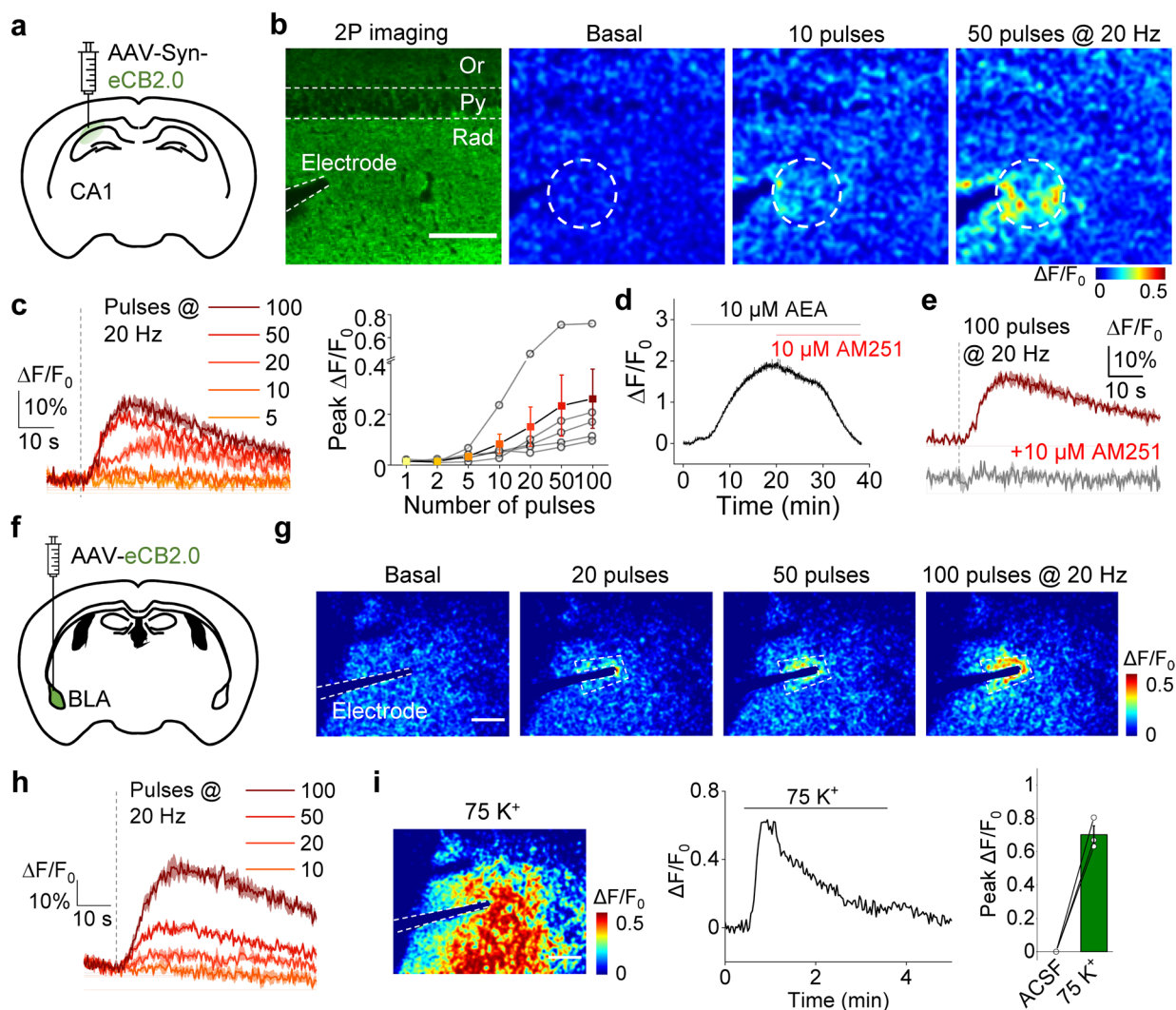


Extended Data Fig. 6 | Spontaneous eCB transients in cultured neurons are sensitive to the CB1R neutral antagonist but not the action potential blocker.

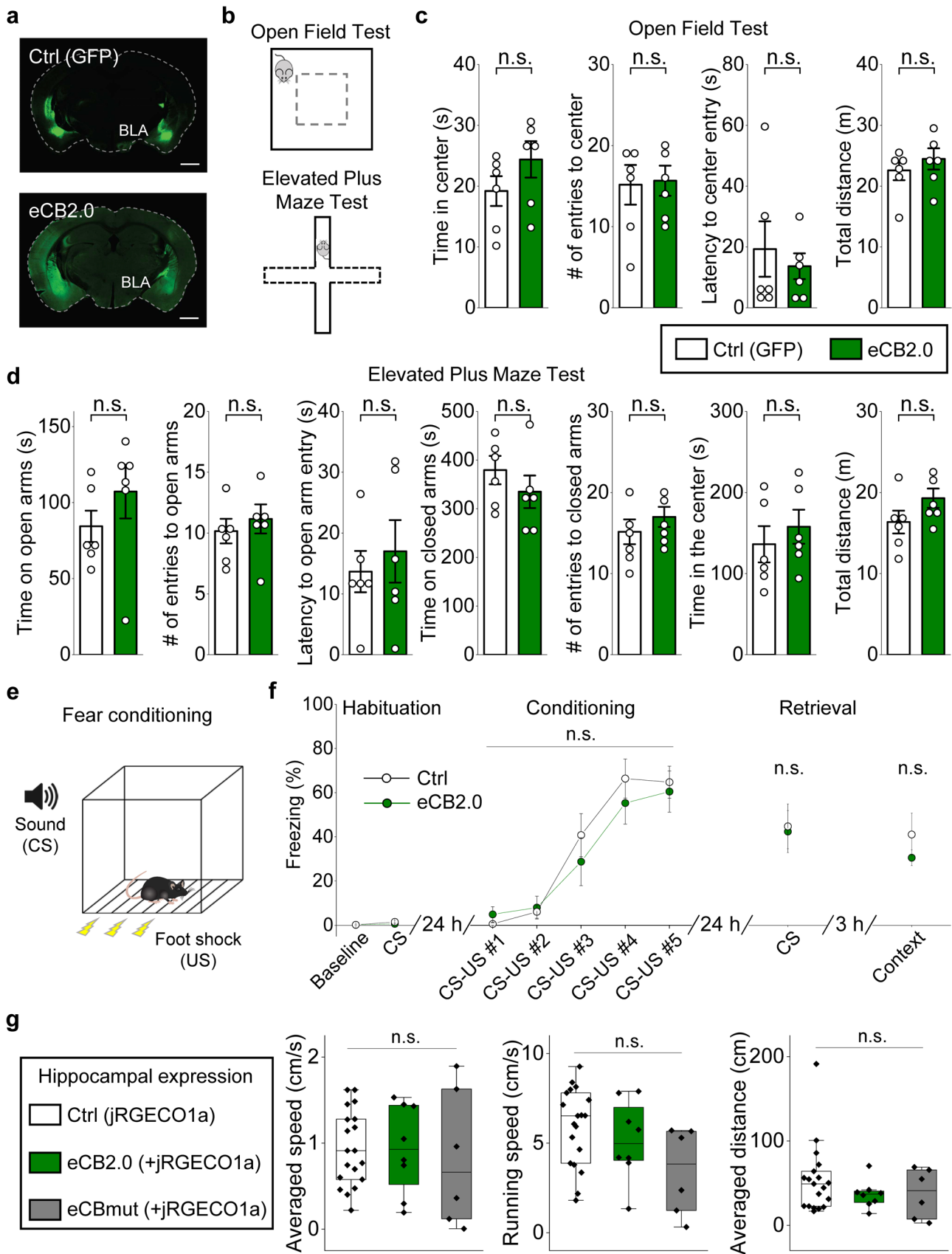
a, Cumulative transient change in eCB2.0 fluorescence measured during 20 mins of recording in the absence (left) or presence (right) of 1 μ M NESS0327. Pseudocolor images were calculated as the average temporal projection subtracted from the maximum temporal projection. Similar results were observed for 3 cultures. Scale bar, 100 μ m. **b**, Summary of the frequency of transient changes in eCB2.0 fluorescence measured in saline (Ctrl) and after NESS0327 application; $n = 18$ & 18 sessions from 3 cultures with 10-min recording/session. Boxes show the first and third quartiles as well as the median (line), and the whiskers extend to the most extreme data point that is no more than 1.5 \times the interquartile range from the box. Two-tailed Student's t test was performed: $P = 1.68E-5$. **c**, Cumulative transient change in eCB2.0 fluorescence measured during 20 mins of recording in the absence (left) or presence (right) of 1 μ M TTX. Pseudocolor images were calculated as the average temporal projection subtracted from the maximum temporal projection. Similar results were observed for 3 cultures. Scale bar, 100 μ m. **d**, Summary of the frequency of transient changes in eCB2.0 fluorescence measured in saline (Ctrl) and after TTX application; $n = 12$ & 14 sessions from 3 cultures with 10-min recording/session. Boxes show the first and third quartiles as well as the median (line), and the whiskers extend to the most extreme data point that is no more than 1.5 \times the interquartile range from the box. Two-tailed Student's t test was performed: $P = 0.5972$. ***, $p < 0.001$; n.s., not significant.



Extended Data Fig. 7 | Detection of 2-AG, AEA, and DSI in GRAB_{eCB2.0} expressed acute striatal slices. **a**, Schematic diagram depicting the strategy for virus injection in DLS, followed by the preparation of acute brain slices used for electrical stimulation and recording. **b**, Schematic diagram depicting the quantification of F_0 and decay time constant of the evoked eCB2.0 signal. **c**, Quantification of relative F_0 and decay time constant of evoked eCB2.0 signals before and after JZL184 or URB597 treatment. $n=3$ slices, mean \pm s.e.m. **d**, Fluorescence microscopy images of control and eCB2.0 expressed striatal slices. Recorded MSN neurons were loaded with Alexa 594. Similar results were observed for more than 10 neurons. Scale bar, 10 μ m. **e**, Depolarizing neurons in control and eCB2.0 expressed striatum caused similar depression on sIPSC. Three shadow regions correspond to baseline, early and late in **c**. **f**, Summary of normalized charge recorded in MSNs in control and eCB2.0 expressed striatum during baseline, right after depolarization (early) and 16 s after depolarization (late); $n=8$ and 13 neurons, mean \pm s.e.m. Two-tailed Wilcoxon matched-pairs signed rank tests were performed: $P=0.0078$ (upper left), 0.0234 (upper right), 0.0134 (bottom left) and 0.0266 (bottom right). **, $p < 0.01$; *, $p < 0.05$.

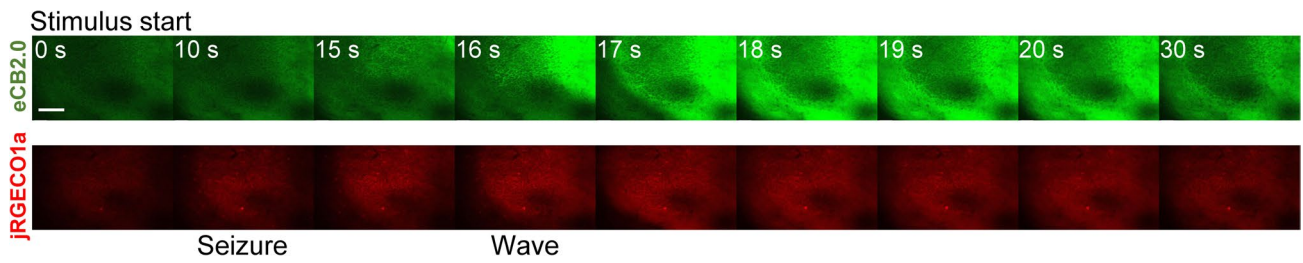


Extended Data Fig. 8 | Detection of eCB signals in acute hippocampal and BLA slices using 2 photon imaging. **a**, Schematic diagram depicting the strategy for virus injection in the hippocampal CA1 region, followed by the preparation of acute slices for electrical stimulation and 2-photon imaging. **b**, (Left) fluorescence image of eCB2.0 expressed in the hippocampal CA1 region, showing the position of the stimulating electrode. (Right) pseudocolor images showing the change in eCB2.0 fluorescence at baseline and after 10 or 50 pulses applied at 20 Hz. The dashed circle shows the ROI for quantification. Similar results were observed for 5 slices. Scale bar, 100 μm . **c**, Representative traces and summary of the peak change in eCB2.0 fluorescence evoked by electrical pulses applied at the indicated frequencies; $n=5$ slices, mean \pm s.e.m. **d**, Time course of the change in eCB2.0 fluorescence; where indicated, AEA and AM251 were applied. **e**, Representative traces of the change in eCB2.0 fluorescence evoked by electrical stimulation in the absence and presence of AM251. **f**, Schematic diagram depicting the strategy for virus injection in the BLA region, followed by the preparation of acute slices for electrical stimulation and 2-photon imaging. **g**, Pseudocolor images showing the change in eCB2.0 fluorescence after 20, 50 or 100 pulses applied at 20 Hz. Similar results were observed for 3 slices. Scale bar, 100 μm . **h**, Traces of eCB2.0 fluorescence evoked by electrical pulses applied at the indicated frequencies. **i**, Representative pseudocolor image, trace, and summary of peak change in eCB2.0 fluorescence upon 75 mM K^+ ACSF perfusion. Scale bar, 100 μm . $n=3$ slices, mean \pm s.e.m.



Extended Data Fig. 9 | See next page for caption.

Extended Data Fig. 9 | Expression of GRAB_{eCB} sensors has minimal effect on animal behaviors. **a**, Fluorescence images of coronal slices prepared from mice expressing GFP or GRAB_{eCB2.0} in BLA. Similar results were observed for 6 mice. Scale bar, 1 mm. **b**, Schematic diagrams showing the open field test (OFT) and the elevated plus maze test (EPMT). **c**, Quantification of behavioral parameters in the OFT. $n = 6$ mice, mean \pm s.e.m. Two-tailed Student's *t* tests were performed: $P = 0.2084, 0.8737, 0.5858$ and 0.4464 . **d**, Quantification of behavioral parameters in the EPMT. $n = 6$ mice, mean \pm s.e.m. Two-tailed Student's *t* tests were performed: $P = 0.2912, 0.5377, 0.6007, 0.3386, 0.3748, 0.4958$ and 0.1411 . **e**, Schematic diagram showing the fear conditioning test. **f**, Quantification of freezing behavior before, during and after conditioning. $n = 6$ mice, mean \pm s.e.m. Two-way ANOVA test was performed: $P = 0.3799$ (between two animal groups during conditioning); two-tailed Student's *t* tests were performed: $P = 0.3297$ and 0.8669 (during retrieval). **g**, Quantification of averaged speed, running speed and averaged distance in control, eCB2.0 and eCBmut expressing mice; $n = 19, 8$ and 6 mice. Boxes show the first and third quartiles as well as the median (line), and the whiskers extend to the most extreme data point that is no more than $1.5\times$ the interquartile range from the box. One-way ANOVA tests were performed: $P = 0.9017, 0.0681$ and 0.4197 . n.s., not significant.



Extended Data Fig. 10 | eCB and Ca^{2+} waves in mouse hippocampal CA1 region during seizure activity. *In vivo* two-photon fluorescence images of eCB2.0 and jRGECO1a expressed in the mouse hippocampal CA1 region before and after stimulus evoked seizure activity. Frames were extracted from those shown in Supplementary Video 1. Seconds (s) after the stimulus are indicated. Similar results were observed for 6 mice. Scale bar, 100 μm .